frontiers in Energy Research

ORIGINAL RESEARCH
published: 07 August 2020
doi: 10.3389/fenrg.2020.00187

Water-Stable High Lithium-Ion Conducting Solid Electrolyte of $Li_{1.4}Al_{0.4}Ge_{0.2}Ti_{1.4}(PO_4)_3$–LiCl for Aqueous Lithium-Air Batteries

Fan Bai[1,2], Kouichi Kakimoto[2], Xuefu Shang[3], Daisuke Mori[2], Sou Taminato[2], Mitsuhiro Matsumoto[2], Yasuo Takeda[2], Osamu Yamamoto[2], Hiroaki Izumi[4]*, Hironari Minami[4] and Nobuyuki Imanishi[2]*

[1] The State Key Laboratory of High Performance Ceramics and Superfine Microstructure, Shanghai Institute of Ceramics, Chines Academy of Science, Shanghai, China, [2] Graduate School of Engineering, Mie University, Tsu, Japan, [3] Department of Physics, Faculty of Engineering, Jiangsu University, Zhenjiang, China, [4] Automobile Electrical Design Department, Suzuki Motor Corporation, Hamamatsu, Japan

OPEN ACCESS

Edited by:
Feifei Shi,
Pennsylvania State University (PSU), United States

Reviewed by:
Qiaobao Zhang,
Xiamen University, China
Yuping Wu,
Fudan University, China

***Correspondence:**
Osamu Yamamoto
yamamoto@chem.mie-u.ac.jp
Hiroaki Izumi
izumh@hhq.susuki.co.jp

Specialty section:
This article was submitted to Electrochemical Energy Conversion and Storage, a section of the journal Frontiers in Energy Research

Received: 16 April 2020
Accepted: 15 July 2020
Published: 07 August 2020

Citation:
Bai F, Kakimoto K, Shang X, Mori D, Taminato S, Matsumoto M, Takeda Y, Yamamoto O, Izumi H, Minami M and Imanishi N (2020) Water-Stable High Lithium-Ion Conducting Solid Electrolyte of $Li_{1.4}Al_{0.4}Ge_{0.2}Ti_{1.4}(PO_4)_3$–LiCl for Aqueous Lithium-Air Batteries. Front. Energy Res. 8:187. doi: 10.3389/fenrg.2020.00187

Aqueous lithium-air batteries are one of the most promising batteries for electric vehicles because of its high energy and power density. The battery system consists of a lithium anode and an aqueous solution catholyte, which are separated by a water-stable lithium-ion-conducting solid electrolyte, and an air electrode. The theoretical energy density of this system is 1,910 W h kg^{-1}, which is around five times higher than that of conventional lithium-ion batteries. A key component of this system is the water-stable lithium-ion-conducting solid electrolyte. In this work, we have developed a water-stable and water-impermeable solid electrolyte with a high lithium-ion conductivity of around 10^{-3} S cm^{-1} at room temperature by the addition of epoxy resin and LiCl into a tape-cast NASICON-type $Li_{1.4}Al_{0.4}Ge_{0.2}Ti_{1.4}(PO_4)_3$ film. The aqueous lithium-air battery with the solid electrolyte separator was successfully cycled at 0.5 mA cm^{-2} and 25°C in an air atmosphere.

Keywords: solid electrolyte, lithium-ion conductor, NASICON type, aqueous lithium air, energy storage

INTRODUCTION

Several types of high-energy-density batteries, such as lithium–sulfur (Yamin et al., 1988; Shim et al., 2002), non-aqueous lithium-air (Abraham and Jiang, 1996; Lu et al., 2014; Gao et al., 2017), aqueous lithium-air (Visco et al., 2004; Zhang et al., 2010), and all-solid-state (Takada, 2013; Kato et al., 2016) batteries have been extensively studied in the last few decades. The non-aqueous lithium-air system has the highest theoretical specific energy density, which is as high as 3,505 W h kg^{-1} and 3,436 W h L^{-1}; however, this system requires an air purification system or oxygen tank (Gallagher et al., 2014). The lithium–sulfur system, which has high specific energy densities of 2,567 W h kg^{-1} and 2,199 W h L^{-1}, has a serious problem of dissolution of the reaction product into the electrolyte (Bruce et al., 2012). All-solid-state batteries have inherent safety, a wide operable temperature range, and potential benefits in terms of the power density; however, the estimated specific energy density is only slightly higher than that of the conventional lithium-ion battery (Kato et al., 2016). The

aqueous lithium-air battery is one attractive candidate for application as the power source in electric vehicles because of its high energy and power densities. The theoretical energy densities of the aqueous lithium-air battery are 1,910 W h kg^{-1} and 2,004 W h L^{-1}, which are lower than those of non-aqueous lithium-air batteries but five and two times higher than those of the conventional lithium-ion batteries in terms of mass and volume, respectively (Yamamoto, 2014). The aqueous system with an acidic catholyte does not require a water purification system (Zhang et al., 2010; Soga et al., 2020). As the cell reaction product in this system is soluble in the catholyte, a high-power-density aqueous lithium-air batteries were reported (Imanishi and Yamamoto, 2019). The aqueous lithium-air battery consists of a lithium anode, a lithium-stable interlayer electrolyte, a water-stable lithium conducting solid electrolyte separator, an aqueous catholyte, and an air electrode. Some other types of lithium aqueous batteries with a similar water-stable lithium-ion-conducting solid electrolyte were also proposed by many groups. Goodenough and colleagues (Lu et al., 2011) proposed an aqueous lithium battery with a lithium anode and an aqueous $Fe(CN)_6^{3-}/Fe(CN)_6^{4-}$ redox couple, and Imanishi and colleagues (Morita et al., 2017, 2018; Watanabe et al., 2019) proposed an aqueous lithium battery with a lithium anode and an aqueous MCl_2/M (M = Sn, Co, and Ni) redox couple. Wu and colleagues reported a lithium battery using an aqueous electrolyte solution with a lithium anode and a $LiFePO_4$ (Hou et al., 2013; Chang et al., 2016), $LiCoO_2$ (Wang et al., 2013b), or $LiMn_2O_4$ (Wang et al., 2013a) cathode. The lithium anode and the catholyte were separated by a water-stable NASICON-type lithium-ion conducting solid electrolyte. The key material of these systems are the solid electrolyte separator. The requirements of the solid electrolyte separator are as follows: high lithium-ion and low electron conductivity, stability in contact with lithium metal, ease of thin film preparation, excellent mechanical properties, and stability in contact with water. Several types of the water-stable high lithium-ion-conducting solid electrolytes have been reported, such as NASICON-type $Li_{1+x}Al_xTi_{2-x}(PO_4)_3$ (LATP) (Aono et al., 1990), garnet-type $Li_7La_3Zr_2O_{12}$ (LLZ) (Murugan et al., 2007), and perovskite-type $La_{2/3-x}Li_{3x}TiO_3$ (LLTO) (Inaguma et al., 1993). LLZ is stable in contact with lithium; however, the Li/LLZ/Li cell showed short circuit at a low current density of 0.5 mA cm^{-2} for a short period of polarization (Sudo et al., 2014). LATP and LLTO are unstable in contact with lithium (Imanishi et al., 2008); therefore, these solid electrolytes require a lithium-stable interlayer between the lithium metal anode and the water-stable solid electrolyte. Li_3N (Visco et al., 2004), a polymer electrolyte (Zhang et al., 2010), lithium phosphorus oxynitride (Stevens et al., 2010), and a conventional non-aqueous liquid electrolyte (Sunahiro et al., 2014) have been used as interlayer materials. LATP is the best candidate for the water-stable lithium-ion-conductive solid electrolyte because of its high conductivity. Lithium-ion conductivity of 7×10^{-4} S cm^{-1} at 25°C was reported for $Li_{1.3}Al_{0.3}Ti_{0.7}(PO_4)_3$ by Aono et al. (1990). The conductivity was enhanced to 1.29×10^{-3} S cm^{-1} by the partial substitution of Ge for Ti in $Li_{1.3}Al_{0.3}Ti_{1.7}(PO_4)_3$ (Zhang et al., 2013). A water-impermeable tape-cast film of $Li_{1.4}Al_{0.4}Ti_{1.6}(PO_4)_3$ was prepared by the addition of epoxy resin (Takahashi et al., 2012a). The lithium-ion conductivity of the film with epoxy resin was 4×10^{-4} S cm^{-4} at 25°C. Here, a water-stable and water-impermeable high lithium-ion-conducting solid electrolyte has been developed by the addition of epoxy resin with LiCl into a $Li_{1.4}Al_{0.4}Ge_{0.2}Ti_{1.4}(PO_4)_3$ (LAGTP) tape-cast film. Enhancement of the lithium-ion conductivity by the addition of LiCl into LATP was previously reported by Takahashi et al. (Takahashi et al., 2012b); however, it was dependent on the atmospheric moisture and was not water impermeable. The charge and discharge performance of a Li/interlayer electrolyte/LAGTP with epoxy and LiCl/saturated LiCl and LiOH aqueous solution/carbon, air cell has been demonstrated.

EXPERIMENTAL

LAGTP powders were prepared by the conventional solid-state reaction method as reported in a previous paper

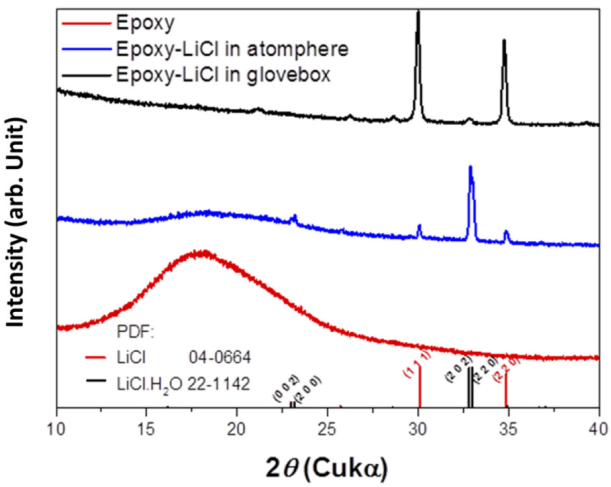

FIGURE 1 | X-ray diffraction (XRD) patterns of epoxy resin, epoxy resin with LiCl prepared under an air atmosphere, and epoxy resin with LiCl prepared in Ar-filled glove box.

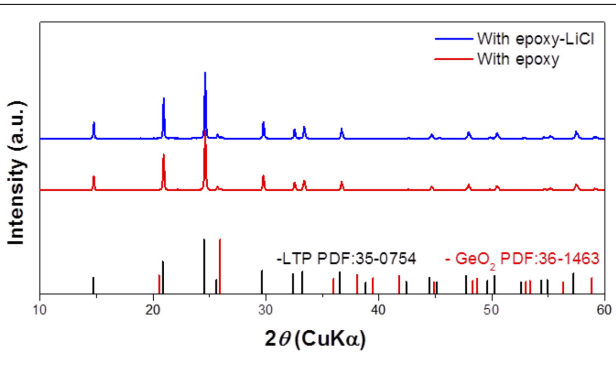

FIGURE 2 | X-ray diffraction (XRD) patterns of LAGTP, LAGTP-E, and LAGTP-E-LiCl.

(Shang et al., 2016). Corresponding amounts of Li_2CO_3, TiO_2, Al_2O_3, $NH_4H_2PO_4$ (Nakalai Tesque, Japan), and GeO_2 (Sigma Aldrich) were ball milled in isopropanol with zirconia balls in a zirconia vessel using a planetary micromill (Fritsch Pulverisette 7). The mixture was dried before calcination at 600°C for 5 h. The calcined powders were then ball milled again. The obtained powders were isostatically pressed into pellets at 150 MPa and sintered at 800°C for 4 h. The tape-cast LAGTP films were prepared using a previously reported method (Bai et al., 2019). A mixture of LAGTP powder, menhaden fish oil as a dispersant (Sigma Aldrich), benzyl-butyl-phthalate as a plasticizer (Wako Chemical, Japan), and polyvinyl butyral as a binder (Butvar B98, Sigma Aldrich) in a toluene and ethanol mixed solvent (1:1 v/v) was ball milled. The slurry was debubbled in a planetary

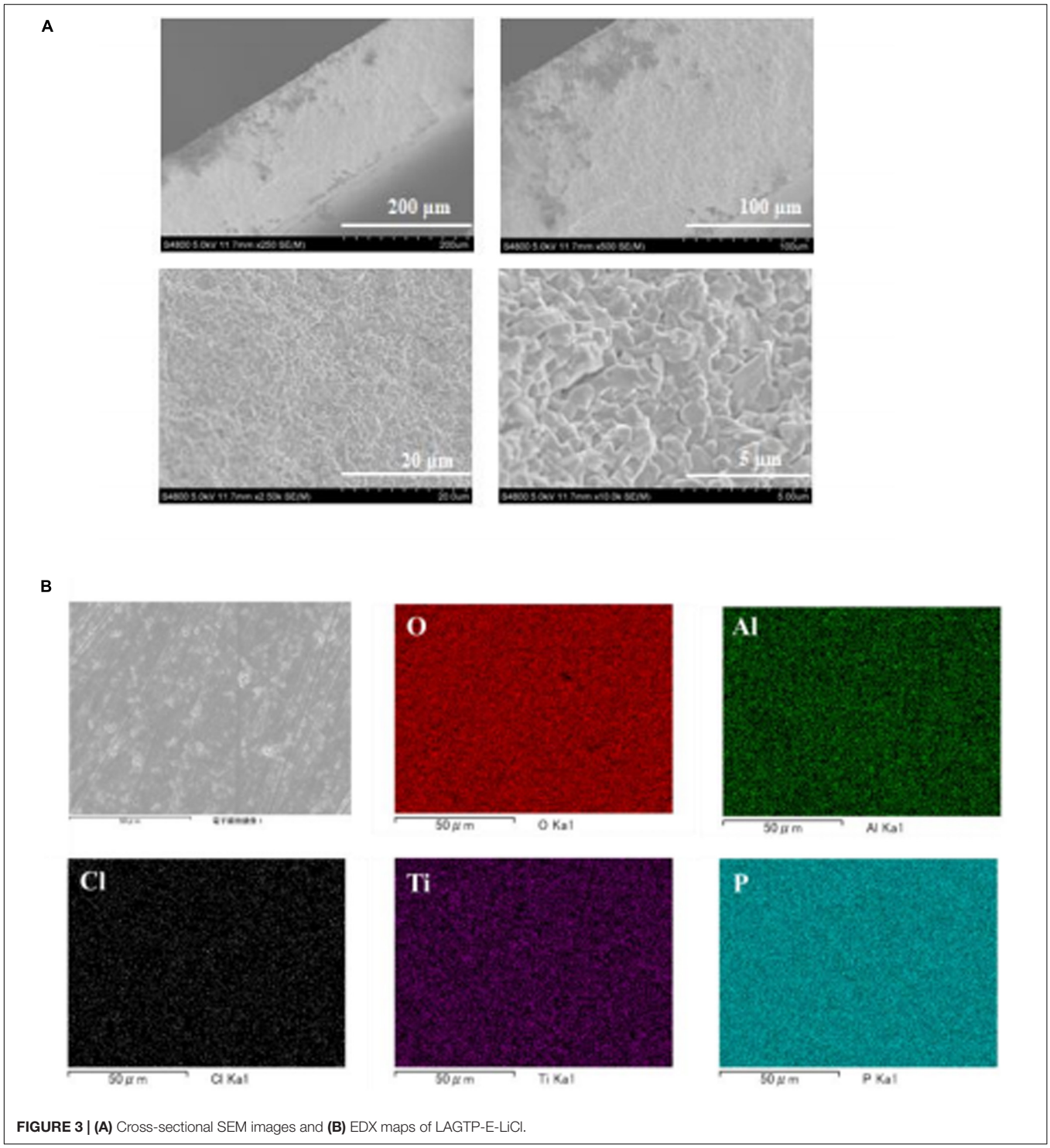

FIGURE 3 | (A) Cross-sectional SEM images and **(B)** EDX maps of LAGTP-E-LiCl.

vacuum mixer (Thinky, Japan) before casting on a silicon-coated polyethylene substrate using a two-doctor-blade apparatus. The green tape-cast sheets were kept in a sealed box with a small amount of ethanol in a refrigerator to slow down the drying process at 4°C for 24 h. The green sheet was punched into disks with a typical diameter of 20 mm and a thickness of around 40 μm. Several disks were isostatically hot pressed at 150 MPa and 80°C for 30 min. The disks were calcined at 500°C to remove organic additives and then sintered at 900°C for 7 h. The thickness of the sintered disk was 200–300 μm for both conductivity measurements and for use as the separator in the aqueous lithium-air cell. LAGTP with epoxy resin and LiCl (LAGTP-E-LiCl) was prepared as follows. The LAGTP disks were immersed in a tetrahydrofuran (THF) solution of 0.1 M 1,3-phenylenediamine (Sigma Aldrich) and 2,2-bis(4-glycidyloxy-phenyl)propane (Sigma Aldrich) (0.5:1 molar ratio) with saturated LiCl for 24 h. The content of LiCl in the LiCl saturated solution was ∼11 g L^{-1}. These procedures were conducted in open air. The disks were heated at 60°C for 8 h in open air to evaporate THF and absorb moisture and then heated at 170°C for 24 h to polymerize the epoxy resin. The molecular weight of the epoxy resin was around 2,000 (Bogdal et al., 2002). These drying and polymerization processes were also conducted in an Ar-filled glove box to examine the effect of water.

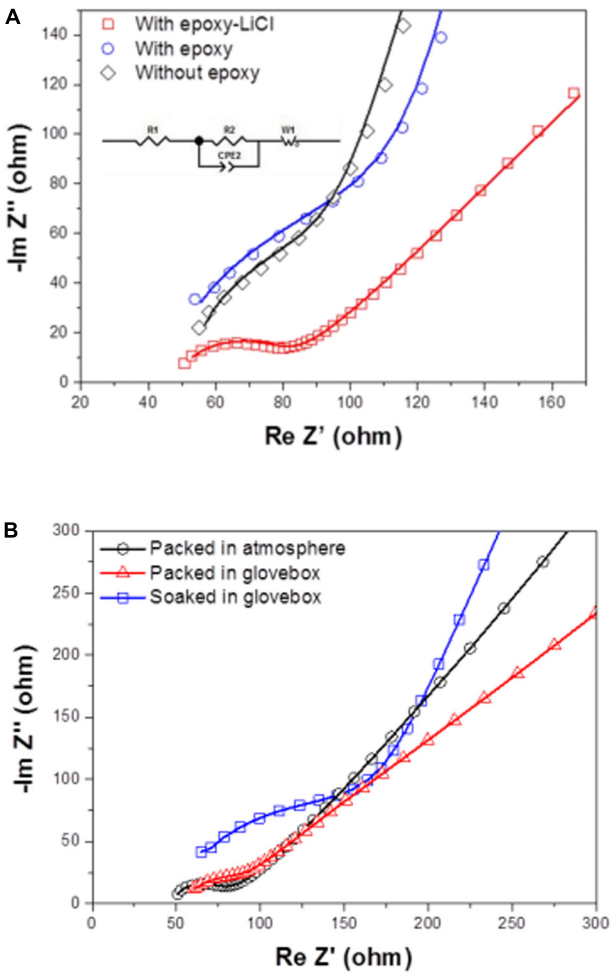

FIGURE 4 | Impedance profiles measured at 25°C of **(A)** Au/LAGTP/Au, Au/LAGTP-E/Au, and Au/LAGTP-E-LiCl/Au packed in plastic envelops under an air atmosphere, and of **(B)** Au/LAGTP-E-LiCl/Au packed under an air atmosphere (○) and in Ar-filled glove box (△), where LAGTP was soaked in a tetrahydrofuran (THF) solution of the epoxy precursor with saturated LiCl under air atmosphere, and Au/LAGTP-E-LiCl/Au packed in an Ar-filled glove box (□), where LAGTP was soaked in a THF solution of the epoxy precursor with saturated LiCl in an Ar-filled glove box.

The phases of epoxy resin, epoxy resin with LiCl, LAGTP, LAGTP with epoxy (LAGTP-E), and LAGTP-E-LiCl were examined by X-ray diffraction (XRD) diffraction analysis (Bruker D8) with Cu Kα radiation. A sintered disk with gold-sputtered electrodes was packed in a vacuum-sealed plastic film. The electrical conductivities of the sintered disks with gold-sputtered electrodes were then measured using an impedance phase analyzer (Solartron 1260) in the frequency range of 0.1 Hz to 1 M Hz with a bias voltage of 10 mV. Bulk and grain boundary conductivities of the samples were estimated from complex impedance plots using Zview 2 (Scribner Associates). Water penetration tests were conducted with an H-type cell and saturated aqueous LiCl solution, the solid electrolyte and distilled water. The water permeation rate through the disk was estimated from the change in the chloride concentration in the distilled water over time using a chloride ion meter (Kasahara Chemical Instruments, Japan). The epoxy resin content was estimated from the weight change after LAGTP soaking in the epoxy precursor solution. The fine powder of LAGTP-E-LiCl was dispersed in 2 M sulfuric acid to determine the LiCl content in the sample. The concentration of chloride ions in 2 M sulfuric acid was determined using a chloride ion meter, and the LiCl content in the sample was then estimated. The morphology and element distribution of the sintered disks were characterized using scanning electron microscopy (SEM; Hitachi S480) equipped with energy dispersive X-ray spectroscopy (EDX).

The aqueous lithium-air cell performance was examined using an in-house-built Swagelok-type cell (Sunahiro et al., 2014). The cell consisted of a 200-μm thick lithium metal anode (Honjyo Metal), a {[$Li(FSO_2)_2N$ (LiFSI)-2 tetraglyme (G4)]-50

TABLE 1 | Conductivity data of LAGTP-E-LiCl at 25°C.

Sample	Bulk mS cm^{-1}	Grain boundary mS cm^{-1}	Total mS cm^{-1}
LAGTP*	1.35	1.82	0.77
LAGTP-epoxy*	1.19	0.69	0.44
LAGTP-epoxy-LiCl*	1.36	2.50	0.88
LAGTP-epoxy-LiCl**	1.11	2.11	0.72
Partly in glove box			
LAGTP-epoxy-LiCl*** in glove box	1.02	0.74	0.43

**Samples were prepared under an air atmosphere and conductivity measurement cells were constructed under an air atmosphere. **Samples were prepared under an air atmosphere and conductivity measurement cells were constructed in an Ar-filled glove box. ***All procedures were performed in an Ar-filled glove box.*

vol% 1,3 dioxolane (DOL)} interlayer electrolyte, LAGTP-E-LiCl, a saturated aqueous LiOH solution and saturated LiCl aqueous solution mixture (1:1 v/v) catholyte, and a Ketjen black (KB; Akzo Noble) and polytetrafluoroethylene (PTFE) mixed air electrode pressed on Ti mesh. The (LiFSI-2G4)–50 vol% DOL interlayer was reported to suppress lithium dendrite formation (Wang et al., 2017).

RESULTS AND DISCUSSION

An epoxy resin precursor THF solution with saturated LiCl was heated at 170°C. The procedure was conducted in an Ar-filled glove box or in the open atmosphere to evaluate the effect of water. **Figure 1** shows XRD patterns of epoxy resin and epoxy resins with LiCl prepared in an air atmosphere or in an Ar-filled glove box (dew point about −105°C). The epoxy resins with LiCl prepared in an air atmosphere showed mixed diffraction lines assigned to LiCl and $LiCl{\cdot}H_2O$, while the epoxy resins with LiCl prepared in an Ar-filled glove box showed only trace diffraction lines due to $LiCl{\cdot}H_2O$. This indicates that LiCl was transformed to $LiCl{\cdot}H_2O$ by reaction with water in the atmosphere. **Figure 2** shows XRD patterns of LAGTP-E and LAGTP-E-LiCl prepared in air. Almost all the diffraction lines were indexed by the NASICON-type $LiTi_2(PO_4)_3$ structure, and trace diffraction lines due to GeO_2 were observed as reported previously (Bai et al., 2019). No diffraction lines of LiCl or $LiCl{\cdot}H_2O$ were observed. The ball-milled powder of LAGTP-E-LiCl was dispersed in 2 M sulfuric acid overnight, and the Cl^- content in the solution was measured using a Cl^- ion meter. The content of LiCl in LAGTP-E-LiCl was estimated to be 0.9 wt%. **Figure 3** shows SEM images and elemental distribution maps of the LAGTP-E-LiCl cross-sections. These results indicate that the element distributions were homogeneous, and LiCl may be homogeneously distributed over the sample at the grain boundaries.

Figure 4A shows impedance profiles of LAGTP, LAGTP-E, and LAGTP-E-LiCl at 25°C. The processes of soaking and packing for the conductivity measurement cell were conducted in an air atmosphere. The LiCl and epoxy contents were around 0.9 and 1.9 wt%, respectively. The impedance profiles showed a semicircle followed by a straight line. The semicircle is attributed to the grain boundary impedance and the straight line to the diffusion process through the electrode (Bruce and West, 1983). The intercept of the semicircle on the real axis at high frequency represents the bulk resistance (R_1), and the diameter of the semicircle is attributed to the grain boundary resistance (R_2). The calculated bulk, grain boundary, and total conductivities at 25°C using the equivalent circuit shown in **Figure 4A** are summarized in **Table 1**. The total and grain boundary conductivities of LAGTP are comparable to those reported previously (Bai et al., 2020). The total conductivity of LAGTP was decreased from 7.7×10^{-4} to 4.4×10^{-4} S cm^{-1} at 25°C by the addition of epoxy resin. The bulk conductivity was not changed, and the grain boundary conductivity was decreased by the addition of epoxy resin because the high resistivity epoxy resin at grain boundaries suppresses lithium-ion diffusion through the grain boundaries. The LAGTP with epoxy resin and LiCl showed a high total conductivity of 8.8×10^{-4} S cm^{-1} at 25°C, where the bulk conductivity was comparable to that of LAGTP without LiCl, but the grain boundary conductivity was obviously higher than those of either LAGTP or LAGTP-E. As shown in **Figure 1**, the epoxy and LiCl mixture contained the $LiCl{\cdot}H_2O$ phase; therefore, LAGTP-E-LiCl may have $LiCl{\cdot}H_2O$ at grain boundaries. Takahashi et al. (2012b) reported that LAGTP pellets immersed in saturated LiCl aqueous solution and dried at 220°C for 12 h under vacuum exhibited high conductivity of 9.2×10^{-3} S cm^{-1} at 25°C under an air atmosphere (RH of ~50%) and a conductivity of 7×10^{-4} S cm^{-1} at 25°C in an Ar-filled glove box, where the LiCl content was 1.45 wt%. The high conductivity in the air atmosphere was explained by the formation of a low-resistive $LiCl{\cdot}xH_2O$ phase. As shown

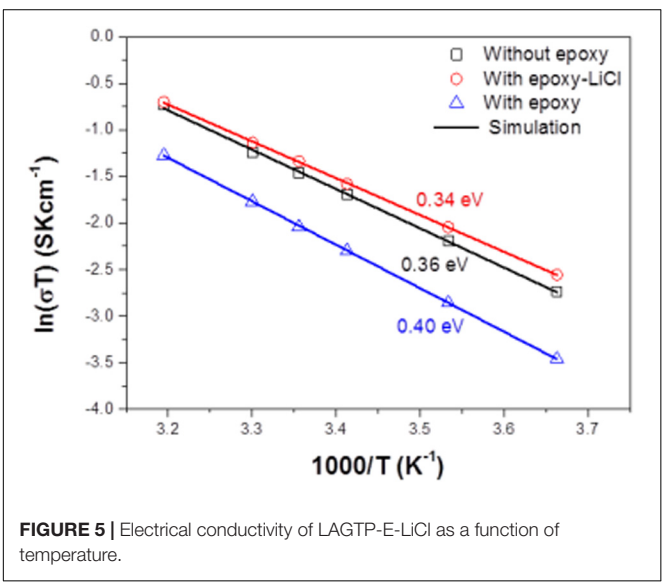

FIGURE 5 | Electrical conductivity of LAGTP-E-LiCl as a function of temperature.

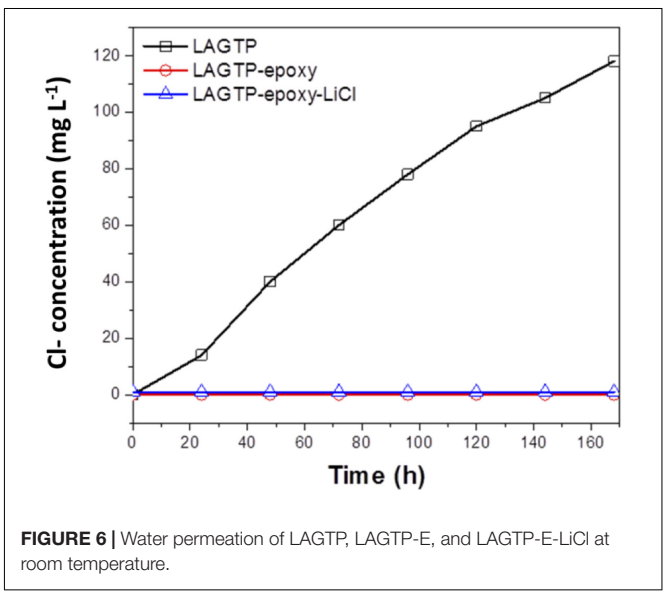

FIGURE 6 | Water permeation of LAGTP, LAGTP-E, and LAGTP-E-LiCl at room temperature.

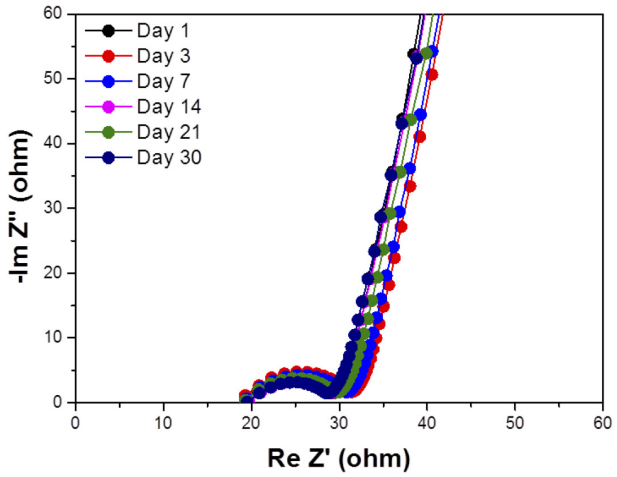

FIGURE 7 | Impedance profiles of symmetric stainless steel (SUS)/saturated LiOH and LiCl aqueous solution/LAGTP-E-LiCl/saturated LiOH and LiCl aqueous solution/symmetric stainless steel (SUS) at 25°C as a function of the storage period.

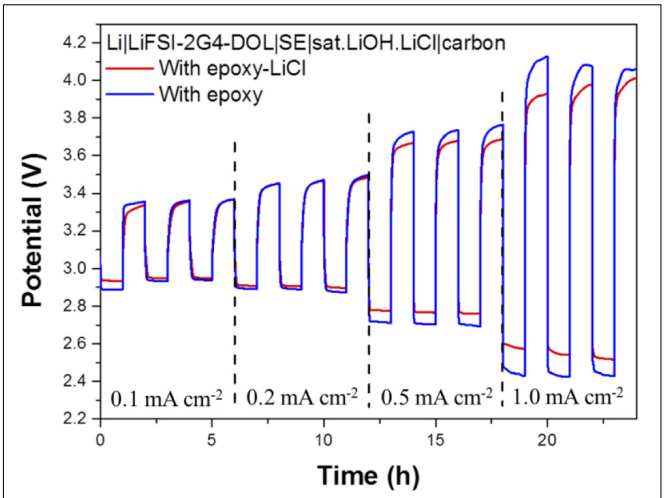

FIGURE 9 | Charge and discharge curves of the Li/(LiFSI-2G4)–50 vol% DOL/LAGTP or LAGTP-E-LiCl/saturated LiOH and LiCl aqueous solution/KB, air cell at various current densities and 25°C.

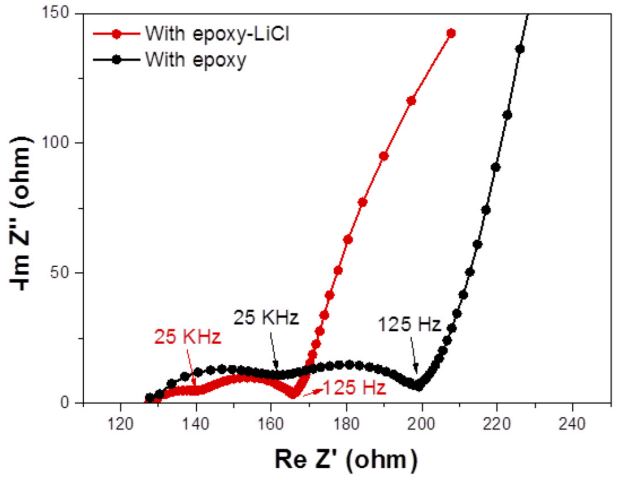

FIGURE 8 | Impedance profiles of the Li/(LiFSI-2G4)–50 vol% DOL/LAGTP-E-LiCl or LAGTP-E/saturated LiOH and LiCl aqueous solution/KB, air cells at 25°C.

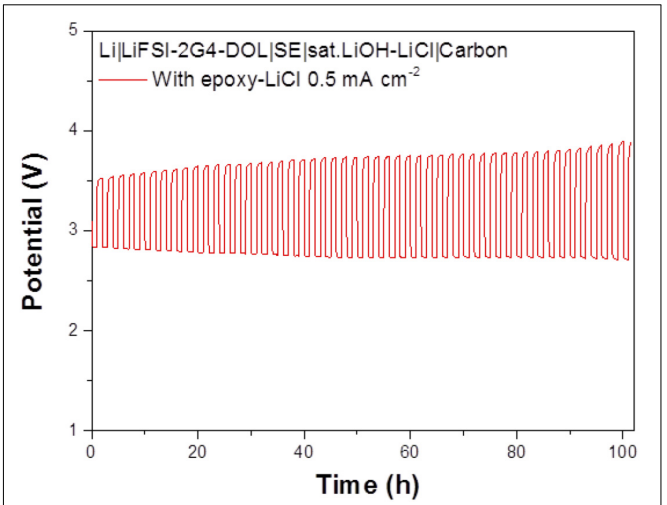

FIGURE 10 | Cycle performance of the Li/(LiFSI-2G4)–50 vol% DOL/LAGTP with epoxy resin and LiCl/saturated LiOH and LiCl aqueous solution/KB, air cell at 0.5 mA cm^{-2} and 25.

in **Figure 1**, epoxy resin with LiCl prepared in the air showed $LiCl{\cdot}H_2O$ and LiCl while that prepared in an Ar-filled glove box showed LiCl with only trace $LiCl{\cdot}H_2O$. To examine the effect of water on the conductivity, the impedance of LAGTP-E-LiCl prepared in an Ar-filled glove box was compared with LAGTP-E-LiCl prepared in air. The impedances of Au/LAGTP-E-LiCl/Au cells assembled in air and in an Ar-filled glove box were also compared. **Figure 4B** shows impedance profiles of these cells at 25°C. The lithium-ion conductivity of LAGTP-E-LiCl assembled in an Ar-filled glove box is slightly lower than that assembled in air, where LAGTP was soaked in the epoxy and LiCl solution in air. The lithium-ion conductivity of LAGTP-E-LiCl assembled in an Ar-filled glove box using LAGTP-E-LiCl soaked in the epoxy and LiCl solution in an Ar-filled glove box was comparable to that of LAGTP-E, which suggests that small amount of LiCl (0.9 wt%) has no effect on the lithium-ion conductivity of LAGTP-E. The enhancement of conductivity by the addition of both epoxy resin and LiCl could be explained by $LiCl{\cdot}H_2O$ at the grain boundaries. **Figure 5** shows the temperature dependence of the lithium-ion conductivity for LAGTP-E-LiCl (1.9 wt% epoxy resin and 0.9 wt% LiCl), LAGTP-E (1.9 wt% epoxy resin), and LAGTP. The activation energy for the conduction of LAGTP, 0.36 eV, was slightly higher than 0.30 eV (Zhang et al., 2013) reported previously for a sintered LAGTP pellet. The lowest activation energy for conduction of 0.34 eV was observed for LAGTP-E-LiCl, and the highest was 0.4 eV for LAGTP-E. The higher activation energy for LAGTP-E

may be due to the higher resistivity of the grain boundary phases with epoxy resin.

Water impermeability through the solid electrolyte as a separator for aqueous lithium-air batteries is an important requirement because if water in the catholyte passes through the solid electrolyte, the lithium metal anode will react with water. **Figure 6** shows the test results of water permeation for LAGTP, LAGTP-E, and LAGTP-E-LiCl at room temperature. The LAGTP disk (∼0.25 mm thick) without epoxy resin showed a linear increase of the Cl^- content with time, while no water permeation was observed for the LAGTP-E and LAGTP-E-LiCl disks (∼0.25 mm thick) because the open pores in LAGTP were closed by epoxy resin. The stability of the lithium-ion-conducting solid electrolyte in contact with the catholyte is another important requirement for aqueous lithium-air batteries. The NASICON-type lithium-ion conducting solid electrolyte of $Li_{1+x}Al_xTi_{2-x}(PO_4)_3$ has been reported to be stable in weak acid and weak alkaline solutions with a high content of Li^+ (Shimonishi et al., 2010, 2011; Zhang et al., 2011). The stability of the LAGTP-E-LiCl disk in saturated LiOH and LiCl aqueous solution (∼pH 8), which is a typical catholyte for aqueous lithium-air batteries (Puech et al., 2012; Sunahiro et al., 2014; Safanama and Adams, 2017), was examined using an H-type cell. **Figure 7** shows the impedance profiles of a symmetric stainless steel (SUS)/saturated LiOH and LiCl aqueous solution/LAGTP-E-LiCl/saturated LiOH and LiCl aqueous solution/SUS cell as a function of the storage period. The impedance profiles showed no significant change for 1 month. Therefore, LAGTP-E-LiCl is considered to be stable in the catholyte used for aqueous lithium-air batteries.

The cell performance of the aqueous lithium-air cell with the high lithium-ion conductivity solid electrolyte of LAGTP-E-LiCl was examined at room temperature under an air atmosphere. **Figure 8** shows the impedance profiles of the Li/(LiFSI-2G4)–50 vol% DOL/LAGTP-E-LiCl/saturated LiOH and LiCl aqueous solution/KB, air cell compared with that of a cell with LAGTP-E. These impedance profiles show two semicircles; the semicircle at high frequency corresponds to the grain boundary resistance of the solid electrolyte and that at low frequency to the interface resistance with lithium metal (Nemori et al., 2018). The cell with LAGTP-E-LiCl showed a lower cell resistance of ∼167 Ω compared with that of the cell with LAGTP-E (∼200 Ω), where the contact area of the lithium electrode with the interlayer electrolyte was 1.13 cm^2, that of the interlayer electrolyte with the solid electrolyte was 1.76 cm^2, and that of the catholyte with the air electrode was 2.0 cm^2. The real axis intercept of the high-frequency semicircle corresponds to the sum of the bulk resistance of the solid electrolyte and resistances of the interlayer electrolyte and the catholyte. The lithium-ion conductivity of the interlayer electrolyte was $\sim 5 \times 10^{-3}$ S cm^{-1}at 25°C (Wang et al., 2017), and the thickness of the electrolyte was about 0.5 cm. Therefore, the resistance of the interlayer electrolyte is as high as 100 Ω. The resistance of the cell with LAGTP-E-LiCl could thus be reduced to <100 Ω cm^{-2} if a thin interlayer electrolyte was used. The low cell resistance is an important requirement to achieve a high power density. **Figure 9** shows the charge and discharge performance of the Li/(LiFSI-2G4) – 50 vol% DOL/LAGTP-E or LAGTP-E-LiCl/saturated LiOH and LiCl aqueous solution/KB, air cell at 25°C and various current densities. The open circuit voltage of the cell was 3.08 V, which is slightly higher than that reported previously (Sunahiro et al., 2014). The charge and discharge overpotentials for the cell with LAGTP-E-LiCl were lower than those for the cell with LAGTP-E. The charge and discharge overpotentials were considerably high at a high current density. The lithium deposition and stripping overpotential between lithium and (LiFSI-2G4) – 50 vol% DOL was low (Wang et al., 2017), and the cell resistance was low; therefore, the high overpotential could be attributed to the oxygen reduction and oxygen evolution reactions at the KB electrode (Ohkuma et al., 2013). The round trip energy loss by the overpotential at 0.2 mA cm^{-2} was ∼20%, which is comparable to that for a non-aqueous lithium-air battery at 0.2 mA cm^{-2} under an oxygen atmosphere (Zhang et al., 2017). **Figure 10** shows the discharge and discharge cycle performance (1 h each) of the Li/(LiFSI-2G4)–50 vol% DOL/LAGTP-E-LiCl/saturated LiOH and LiCl aqueous solution/KB, air cell at 0.5 m cm^{-2} and 25°C. The cell was successfully cycled for 50 cycles. The charging voltage was increased slightly with cycling from 3.35 to 3.8 V. The increase may be due to the formation of Li_2CO_3 on the air electrode because the cell was operated under air (Sunahiro et al., 2014).

CONCLUSION

A water-stable and water-impermeable high lithium-ion conductivity solid electrolyte of LAGTP with epoxy resin and LiCl was developed by immersion in an epoxy resin precursor THF solution with saturated LiCl. The epoxy resin and LiCl contents in LAGTP-E-LiCl were estimated to be 1.9 and 0.9 wt%, respectively. The lithium-ion conductivity of LAGTP-E-LiCl at 25°C was 8.8×10^{-4} S cm^{-1}, which was approximately two times higher than that of LAGTP-E without LiCl. The high lithium-ion conductivity in LAGTP-E-LiCl could be explained by the low resistance of the $LiCl{\cdot}H_2O$ phase at the grain boundaries. The Li/(LiFSI-2G4)–50 vol% DOL/LAGTP with epoxy and LiCl/saturated LiOH and LiCl aqueous solution/KB, air cell was successfully cycled at 0.5 m cm^{-2} and 25°C in an air atmosphere.

DATA AVAILABILITY STATEMENT

The raw data supporting the conclusions of this article will be made available by the authors, without undue reservation, to any qualified researcher.

AUTHOR CONTRIBUTIONS

All authors listed have made a substantial, direct and intellectual contribution to the work, and approved it for publication.

REFERENCES

Abraham, K. M., and Jiang, Z. (1996). A polymer electrolyte-based rechargeable lithium oxygen battery. *J. Electrochem. Soc.* 431, 1–5. doi: 10.1149/1.1836378

Aono, H., Sugimoto, E., Sadaoka, Y., Imanaka, N., and Adachi, G. (1990). Ionic conductivity of solid electrolytes based on lithium titanium phosphate. *J. Electrochem. Soc.* 137, 1023–1027. doi: 10.1149/1.2086597

Bai, F., Mori, D., Taminato, S., Takeda, Y., Yamamoto, O., Nemori, H., et al. (2020). Electrical and mechanical properties of water-stable NASICON-type Li1+AlxGe0.2Ti1.8-x(PO4)3. *Solid State Ionics* 345:115151. doi: 10.1016/j.ssi.2019.115151

Bai, F., Shan, X., Mori, D., Taminato, S., Matsumoto, M., Watanabe, S., et al. (2019). High lithium-ion conducting solid electrolyte thin film of Li1.4Al0.4Ge0.2Ti1.4(PO4)3-TiO2 for aqueous lithium secondary batteries. *Solid State Ionics* 338, 127–133. doi: 10.1016/j.ssi.2019.05.017

Bogdal, D., Pielichowski, J., Penczr, P., Gorczvk, J., and Kowalski, G. (2002). Synthesis of elevated-molecular-weight epoxy resins with aid of microwaves. *Polimery* 47, 11–12.

Bruce, P. G., Freunberger, S. A., Hardwick, L. J., and Tarascon, J.-M. (2012). LiO2 and Li-S batteries with high energy storage. *Nat. Mater.* 11, 19–29. doi: 10.138/nmat.3191

Bruce, P. G., and West, A. R. (1983). The AC conductivity of polycrystalline LISICON Li2+2xZn1-xGeO4 and a model for intergranular constriction resistance. *J. Electrochem. Soc.* 130, 662–669. doi: 10.1149/1.12119778

Chang, Z., Li, C., Wang, Y., Chen, B., Fu, L., Zhu, Y., et al. (2016). A lithium ion battery using an aqueous electrolyte solution. *Sci. Rep.* 6:28421. doi: 10.1038/srep28421

Gallagher, K. G., Goebel, S., Greszler, T., Mathias, M., Oelerich, W., Eroglu, D., et al. (2014). Quantifying the promise of lithium-air batteries for electric vehicles. *Energy Environ. Sci.* 7, 1555–1563. doi: 10.1039/c3ee43870h

Gao, X., Chen, Y., Johnson, L. R., Javanov, Z. P., and Bruce, P. G. (2017). A reversible lithium-oxygen battery with dual mediator stabilizing the carbon cathode. *Nat. Energy* 2, 17118–17120. doi: 10.1038/nenergy.2017118

Hou, Y., Wang, X., Zhu, Y., Hu, C., Chang, Z., Wu, Y., et al. (2013). Microporous LiFePO4 as a cathode for an aqueous rechargeable lithium battery of high energy density. *J. Mater. Chem. A.* 46, 14713–14718. doi: 10.1039/c3ta13472e

Imanishi, N., Hasegawa, S., Zhang, T., Hirano, A., Takeda, Y., and Yamamoto, O. (2008). Lithium anode for lithium-air secondary batteries. *J. Power Sources* 185, 1392–1397. doi: 10.1016/j.powsour.2008.07.080

Imanishi, N., and Yamamoto, O. (2019). Perspectives and challenges of rechargeable lithium-air batteries. *Mater. Today Adv.* 4:100031. doi: 10.1016/j.matadv.2019.100031

Inaguma, Y., Ito, M., Uchida, T., Ikuta, H., and Wakihara, M. (1993). High ionic conductivity in lithium lanthanum titanate. *Solid State Commun.* 86, 689–693. doi: 10.1016/0038-1098(93)90841-A

Kato, K., Hori, S., Suzuki, K., Hirayama, M., Mitsui, A., Yomenura, M., et al. (2016). High power all-solid-state batteries using sulfide superionic conductors. *Nat. Energy* 1, 1603–1609. doi: 10.1038/NENERGY.2016.30

Lu, J., Li, L., Park, J. B., Sun, Y.-K., Wu, F., and Amine, K. (2014). Aprotic and aqueous Li-O2 batteries. *Chem. Rev.* 114, 5611–5640. doi: 10.1021/cr400573b

Lu, Y., Goodenough, J. B., and Kim, Y. (2011). Aqueous cathode for next-generation alkali-ion batteries. *J. Amer. Chem. Soc.* 133, 5756–5759. doi: 10.1021/ja201118f

Morita, Y., Watanabe, D., Mori, D., Takeda, Y., Yamamoto, O., and Imanishi, N. (2018). High energy-density rechargeable lithium-nickel chloride aqueous solution batteries. *ACS Omega* 3, 5558–5562. doi: 10.1021/acsomega8b00184

Morita, Y., Watanabe, D., Zhang, P., Wang, H., Mori, D., Matsuda, Y., et al. (2017). High specific energy density aqueous lithium-metal chloride rechargeable batteries. *J. Electrochem. Soc.* 164, A1958–A1964. doi: 10.1149/2.0881709jes

Murugan, R., Tangadurai, V., and Weppner, W. (2007). Fast lithium ion conduction in garnet-type Li7La3Zr2O12. *Angew. Chem. Int. Ed.* 46, 7778–7781. doi: 10.1002/anie.200701144

Nemori, H., Shang, X., Minami, H., Mitsuoka, S., Nomura, M., Sonoki, H., et al. (2018). Aqueous lithium-air batteries with a lithium-ion conducting solid electrolyte Li1.3Al0.5Nb0.2Ti1.3(PO4)3. *Solid State Ionics* 317, 136–141. doi: 10.1016/j.ssi.2018.01.020

Ohkuma, H., Uechi, I., Imanishi, N., Hirano, A., Takeda, Y., and Yamamoto, O. (2013). Carbon electrode with perovskite-oxide catalyst for aqueous electrolyte lithium-air secondary batteries. *J. Power Sour.* 223, 319–324. doi: 10.1016/j.jpowsour.2012.09.028

Puech, L., Cantau, C., Vinatier, P., Toussaint, G., and Stevens, P. (2012). Elaboration and characterization of a free standing LiSICON membrane for aqueous lithium–air battery. *J. Power Sour.* 214, 330–336. doi: 10.1016/j.jpowsour.2012.04.064

Safanama, D., and Adams, S. (2017). High efficiency aqueous and hybrid lithium-air batteries enabled by Li1.5Al0.5Ge1.5(PO4)3 ceramic anode-protecting embraces. *J. Power Sour.* 340, 294–301. doi: 10.1016/j.jpowsour.2016.11.076

Shang, X., Nemori, N., Mitsuoka, S., Xu, P., Matsui, M., Takeda, Y., et al. (2016). High lithium-ion-conducting NASICON-type Li1+xAlxGeyTi2-x-y(PO4)3 solid electrolyte. *Front. Energy Res.* 4:12. doi: 10.3389/fenrg.2016.00012

Shim, J., Striebel, K. A., and Cairns, E. J. (2002). The lithium/sulfur rechargeable cell; Effect of electrode composition and solvent on cell performance. *J. Electrochem. Soc.* 149, A1321–A1325. doi: 10.1149/1.1503076

Shimonishi, Y., Zhang, T., Imanishi, N., Im, D., Lee, D. J., Hirano, A., et al. (2011). A study on lithium/air batteries-Stability of the NASICON-type lithium ion conducting solid electrolyte in alkaline aqueous solutions. *J. Power Sour.* 196, 5128–5132. doi: 10.1016/j.powsour.2011.02.023

Shimonishi, Y., Zhang, T., Johnson, P., Imanishi, N., Hirano, A., Takeda, Y., et al. (2010). A Study on lithium/air batteries-Stability of NASICON-type glass ceramics in acid solution. *J. Power Sour.* 195, 6187–6191. doi: 10.1016/j.powsour.2009.11.023

Soga, S., Bai, F., Zhang, T., Kakimoto, K., Mori, D., Taminato, S., et al. (2020). Ambient air operation rechargeable lithium-air battery with acetic acid catholyte. *J. Electrochem. Soc.* 167:090522. doi: 10.1149/1945.7111/ab86c4

Stevens, P., Toussinit, G., Caillon, G., Viaud, P., Vinatief, F., Cantau, C., et al. (2010). Development of a lithium air rechargeable battery. *ECS Trans.* 28, 1–12. doi: 10.1149/1.3507922

Sudo, R., Nakata, Y., Ishiguro, K., Matsui, M., Hirano, A., Takeda, Y., et al. (2014). Interface behavior between garnet-type lithium conducting solid electrolyte and lithium metal. *Solid State Ionics* 262, 151–154. doi: 10.1016/j.ssi.2013.09.024

Sunahiro, S., Matsui, M., Takeda, Y., Yamamoto, O., and Imanishi, N. (2014). Rechargeable aqueous lithium-air batteries with an auxiliary electrode for the oxygen evolution. *J. Power Sources* 262, 338–343. doi: 10.1016/j.jpowsour.2014.03.016

Takada, K. (2013). Progress and prospective of solid-state lithium batteries. *Acta Mater.* 61, 759–770. doi: 10.1016/j.actamat.2012.10.034

Takahashi, K., Johnson, P., Imanishi, N., Sammes, N., Takeda, Y., and Yamamoto, O. (2012a). A water-stable high lithium ion conducting Li1.4Ti1.6Al0.4(PO4)3-epoxy resin hybrid sheet. *J. Electrochem. Soc.* 159, A1065–A1069. doi: 10.1149/2.072207jes

Takahashi, K., Ohmura, J., Im, D., Lee, D. J., Zhang, T., Imanishi, N., et al. (2012b). A super high lithium-ion conducting solid electrolyte of grain boundary modified Li1.4Ti1.6Al0.4(PO4)3. *J. Electrochem. Soc.* 159, A342–A348. doi: 10.1149/2.018204jes

Visco, S. J., Nimon, E., Katz, B., Jongahe, L. C. D., and Chu, M. Y. (2004). "Lithium metal aqueous batteries," in *Proceedings of the 12th International Meeting on Lithium Batteries*, Nara.

Wang, H., Matsui, M., Kuwata, H., Sonoki, H., Matsuda, Y., Shang, X., et al. (2017). A reversible dendrite-free high-area-capacity lithium metal electrode. *Nat. Commun.* 8:15106.

Wang, X., Hou, Y., Zhu, Y., Wu, Y., and Holze, R. (2013a). An aqueous rechargeable lithium battery using coated Li metal as anode. *Sci. Rep.* 3:1401. doi: 10.1038/srep01401

Wang, X., Qu, Q., Hou, Y., Wang, F., and Wu, Y. (2013b). An aqueous rechargeable lithium battery of high energy density based on coated Li metal and LiCoO2. *Chem. Commun.* 49, 6179–6181. doi: 10.1039/c3cc42676a

Watanabe, S., Mori, D., Taminato, S., Matsuda, Y., Yamamoto, O., Takeda, Y., et al. (2019). Aqueous lithium rechargeable battery with a Tin(II) chloride aqueous cathode and a water-stable lithium-ion conducting solid electrolyte. *J. Electrochem. Soc.* 166, A539–A545. doi: 10.1149/2.0331904jes

Yamamoto, O. (2014). *Introduction. The Lithium Air Battery: Fundamentals*. New York, NY: Springer, doi: 10.1007/978-1-4988-8062-5_1

Yamin, H., Gorenshtein, A., Penciner, J., and Peled, E. (1988). Lithium sulfur battery. *J. Electrochem. Soc.* 135, 1045–1048. doi: 10.1149/1.2095868

Zhang, B., Sun, Y., Zhao, Y., Kreschmer, C., and Wang, C. (2017). Modified tetrathiafulvalene as an organic conductor for improving performance of Li-O2 batteries. *Angew. Chem. Int. Ed.* 56, 8505–8509. doi: 10.1002/anie.201703784

Zhang, P., Matsui, M., Hirano, A., Takeda, Y., Yamamoto, O., and Imanishi, N. (2013). Water-stable lithium-ion conducting solid electrolyte of the Li1.4Al0.4Ti1.6-xGex(PO4)3 system (x=0-1.0) with NASICON-type structure. *Solid State Ionics* 2013, 175–180. doi: 10.1016/j.ssi.2013.09.022

Zhang, T., Imanishi, N., Shimonishi, Y., Hirano, A., Takeda, Y., Yamamoto, O., et al. (2010). A novel high energy density rechargeable lithium/air battery. *Chem. Commun.* 46, 1661–1663. doi: 10.1039/B920012F

Zhang, T., Imanishi, N., Takeda, Y., and Yamamoto, O. (2011). Aqueous lithium/air rechargeable batteries. *Chem. Lett.* 40, 668–673. doi: 10.1246/cl.2011.668

Conflict of Interest: HI and HM were employed by the company Suzuki Motor Corporation.

The remaining authors declare that the research was conducted in the absence of any commercial or financial relationships that could be construed as a potential conflict of interest.